Systematics of moments of dipole oscillator-strength distributions for atoms of the first and second row*

J. L. Dehmer, Mitio Inokuti, and R. P. Saxon†
Argonne National Laboratory, Argonne, Illinois 60439
(Received 19 March 1975)

The moments $S(\mu)$ and $L(\mu) = dS(\mu)/d\mu$ for $-6 \leq \mu \leq 1$ are derived from comprehensive Hartree-Slater oscillator-stength distributions for He through Ar. For $\mu \leq -2$, these moments are governed by valence excitations only, and therefore exhibit a pronounced periodic variation that repeats in each row. Inner shells begin to contribute appreciably to $S(-1)$, which retains a periodic variation superimposed upon an over-all increase with increasing atomic number Z. For $\mu \geq 0$, the Z dependence of the moments becomes dominated by inner-shell contributions; as μ increases, the over-all increase with Z becomes more rapid. Another perspective of the voluminous data is gained by plotting $\log S(\mu)$ vs μ. The plot reveals three classes of behavior—"tight," "intermediate," and "loose" atoms. Comparisons with experiment and more detailed calculations are made where possible.

I. INTRODUCTION

Many important atomic properties, such as polarizability, total inelastic scattering cross section, and stopping power, depend on moments of the dipole oscillator-strength distribution.[1,2] With the advent of realistic atomic potentials,[3] it is now a routine matter to generate atomic dipole oscillator-strength distributions in the framework of an independent-electron model and to separate the contributions from individual subshells. Indeed, this approach has been employed frequently over the past few years to study atomic properties, primarily partial photoionization cross sections[4–10] and photoelectron angular distributions.[11,12] Unfortunately, the body of data resulting from these calculations is either not comprehensive enough or otherwise inappropriate for our present purpose. Specifically, the sum rules we investigate are rigorously defined only in the dipole approximation. Hence, "oscillator strengths" that include the effects of higher multipoles[8–10] or of retardation, while presumably suitable for the photoeffect cross section, do not suit our needs. Also, in view of the ease of performing Hartree-Slater model calculations, we find this preferable to the dipole oscillator-strength distribution based on the less realistic Thomas-Fermi model.[13] There are, of course, many data based on the Hartree-Slater model and the dipole approximation. However, such studies[4–7] usually omit the discrete part of the spectrum, and one[6,14] of them utilizes a mathematical approximation which distorts the Harteee-Slater oscillator-strength distribution in an unpredictable way.

Therefore, we have calculated a comprehensive set of partial dipole oscillator strengths and the related moments for the atoms of the first two rows of the Periodic Table. The motivation for systematically computing these quantities within the independent-electron approximation is twofold: (i) Owing to the ease of computation, we can treat all atoms in the same way, thus filling in the huge gaps left by experiment and more laborious theoretical calculations. This body of data will exhibit reasonable over-all accuracy (5–30%) and shell effects missing from hydrogenic or Thomas-Fermi[13] calculations. As we show below, one gains a distorted view of the behavior of atomic parameters by considering only the rare gases, which are the most accessible experimentally. (ii) Our scheme also exposes systematic variations in each quantity, which, when analyzed according to its shellwise contributions, reveals the region of space (or the region of the spectrum) that influences the quantity most strongly.

The paper deals with the moments of the oscillator-strength distributions. The distributions themselves, as well as side products of our calculation such as phase shifts for electron scattering by positive ions, are tabulated elsewhere.[15]

II. BACKGROUND AND METHOD

Within the independent-electron model, the spectrum of oscillator strength of each atom results from the sum of contributions from all permitted transitions by each of its electrons. The characterization of one-electron states and description of other assumptions inherent in this model are amply described in Secs. 4.2–4.9 of Fano and Cooper.[2] We shall merely list the basic formulas upon which the calculation is based.

The expression for the oscillator strength per electron of a subshell nl is

$$f(nl \rightarrow n'l') = \tfrac{1}{3} m\hbar^{-2}(E_{n'l'} - E_{nl})(l + l' + 1) \times (2l+1)^{-1}[R(nl, n'l')]^2, \quad (1)$$

where E_{nl} is the initial-state energy, the final-state energy $E_{n'l'}$ belongs to either a discrete or continuous part of the spectrum, and $R(nl, n'l')$ is the radial matrix element

$$R(nl, n'l') = \int_0^\infty r P_{nl}(r) P_{n'l'}(r)\, dr. \quad (2)$$

The radial wave functions $P_{nl}(r)$ are solutions [with the condition $P_{nl}(0) = 0$] of the Schrödinger equation

$$\frac{d^2 P_{nl}}{dr^2} + \frac{2m}{\hbar^2}\left(E_{nl} - V(r) - l(l+1)\frac{\hbar^2}{2mr^2}\right) P_{nl}(r) = 0, \quad (3)$$

and are normalized to unity for $E_{nl} < 0$, and per unit energy range for $E_{nl} \geq 0$. For this work, $V(r)$ is a Hartree-Slater potential taken from the tabulation by Herman and Skillman.[3]

The spectral distribution of oscillator strength per electron for a given subshell is

$$\left(\frac{df}{dE}\right)_{nl} = \sum_{n'l'} f(nl \rightarrow n'l')\,\delta(E_{n'l'} - E_{nl} - E), \quad (4)$$

where E is the excitation energy $\hbar\omega$. The total oscillator-strength distribution is obtained by summing $Z_{nl}(df/dE)_{nl}$ over all occupied subshells of the atom, where Z_{nl} is the occupation number of the subshell.

The moment $S(\mu)$ of the total oscillator-strength distribution and the moment $L(\mu)$ containing the additional weight factor $\ln(E/R)$ are defined by

$$S(\mu) = \int \left(\frac{E}{R}\right)^{\mu} \frac{df}{dE}\, dE, \quad (5)$$

$$L(\mu) = \int \left(\frac{E}{R}\right)^{\mu} \left(\ln\frac{E}{R}\right) \frac{df}{dE}\, dE, \quad (6)$$

where df/dE without the subscript nl denotes the *total* oscillator strength, and R is the Rydberg energy. The integration sign in Eqs. (5) and (6) is used here to include a summation over all allowed discrete transition to unoccupied levels. Note that the exclusion of "virtual" transitions to fully occupied levels is not inherent in the independent-electron model and must be added as a physical constraint.

In this work we restrict the value of μ to the range $-6 \leq \mu \leq 1$. This restriction arises on the one hand because $S(\mu)$ and $L(\mu)$ diverge for $\mu \geq 2.5$. The divergence follows from the (nonrelativistic) asymptotic behavior of the spectral density of oscillator strength for large E,

$$df/dE \sim E^{-7/2}, \quad (7)$$

provided that the atom contains an s electron. In addition, the scheme we used to extrapolate df/dE to high energy proved too inaccurate to give a reliable $S(2)$, which depends primarily on the high-energy part of the spectrum. On the other hand, $S(\mu)$ for $\mu < -6$ are related to measurable quantities only in their minor role in the frequency-dependent refractive index and the Verdet constant [see Eqs. (2.29) and (2.30) of Ref. 2], and hence we truncate at $\mu = -6$. No application of $L(\mu)$ for $\mu \leq -2$ is known.

Notice that $L(\mu)$ is the derivative $dS(\mu)/d\mu$ when $S(\mu)$ is considered as a function of continuous variable μ. For the most part, we consider $S(\mu)$ and $L(\mu)$ for integer values of μ only; however, we discuss in Sec. IV $S(\mu)$ as a continuous function of μ.

The independent-electron model has the advantage that the quantities $S(\mu)$ and $L(\mu)$ can be decomposed into contributions from individual subshells or even into contributions from different processes. For example, we will discuss the anatomy of the total sums in terms of shellwise contributions to these sums, i.e., $S_{nl}(\mu)$ and $L_{nl}(\mu)$ which may be defined by replacing df/dE by $(df/dE)_{nl}$ in Eqs. (5) and (6), respectively. It should be pointed out, however, that in the independent-electron model, shellwise sum rules are defined, but only by including virtual excitations to all occupied levels. (See Secs. 4.9 and 5.2 of Ref. 2.) We have used $S_{nl}(0)$ to check the accuracy of of our numerical work, but since the virtual transitions do not actually occur owing to the exclusion principle, we have excluded them in the partial sums we discuss.

The apportionment of $S(\mu)$ and $L(\mu)$ into the shellwise contributions is a useful concept for qualitative understanding, but becomes imprecise as soon as one goes beyond the independent-particle model and considers (intershell) electron correlation effects. The schematic nature of the shellwise contribution should be borne in mind in every quantitative application. (See Sec. 4.9 of Ref. 2.)

Another useful set of quantities distinguishes between contributions to $S(\mu)$ and $L(\mu)$ resulting from the discrete, autoionizing, and pure-continuum part of the spectrum. We define the discrete contribution, $S_D(\mu)$ and $L_D(\mu)$, as that part of the total sums due to discrete transitions of the valence electrons (outermost subshell). The contribution due to autoionizing transitions $S_A(\mu)$ and $L_A(\mu)$ may be taken as the sum of all other discrete transitions. Finally, the sum of the continuum contributions from each subshell is denoted by $S_C(\mu)$ and $L_C(\mu)$. These quantities, taken individually, obey no sum rules, but nevertheless afford an interesting insight into the syste-

matic variation of $S(\mu)$ and $L(\mu)$ discussed below.

A few remarks about the evaluation of the moment sums are warranted. Because the shell-wise contributions to the sums are of interest in themselves, the moments $S(\mu)$ and $L(\mu)$ were actually evaluated by first computing $S_{nl}(\mu)$ and $L_{nl}(\mu)$ and then summing them. A consistent set of numerical conditions was used for the calculation of the partial oscillator-strength distributions. In each case, the oscillator strength for discrete transitions up to the tenth Rydberg level was calculated. The contribution of the remainder of the Rydberg series was evaluated by use of the single-channel quantum-defect theory. For each subshell, the oscillator strength in the continuum was determined at values of the excitation energy spaced closely enough to ensure numerically accurate evaluation of the integrals in Eqs. (5) and (6). The oscillator-strength distribution was extrapolated to infinite energy by fitting the functional form CE^{-B} (where C and B are positive constants) to the two highest energy values. This form was chosen for numerical convenience and represents no constraint of physical significance. Except for $\mu = 2$, the spectral range of this extrapolation contributed a negligible fraction to the total sums. The energy range of actual numerical evaluation of the continuum oscillator strength was chosen so that each subshell satisfies the criterion $S_{nl}(0) = (1 \pm 0.001)Z_{nl}$. For this purpose, $S_{nl}(0)$ includes contributions from virtual transitions.

III. RESULTS

The results of our calculation are summarized in Tables I and II, where we list the total moments $S(\mu)$ and $L(\mu)$ for $-6 \leq \mu \leq 1$. The breakdown into contributions from individual subshells or into the quantities $S_D(\mu)$, $S_A(\mu)$, $S_C(\mu)$, etc., would be too lengthy for presentation here. Rather, we will treat these more detailed quantities when they illuminate the systematic behavior of a particular total sum.

The present section is organized into six subsections. In each, a closely related subset of the data in Tables I and II is discussed from three points of view: (i) Which region of the spectrum of oscillator strength dominates the moment? (ii) Which subshell(s) dominates this region of the spectrum, and how does this account for the observed Z dependence? (iii) How well does the present calculation agree with other calculations and with available experimental data? The subsections are organized in the following order, based loosely on the amount of comparison data available: III A, $S(-2)$, related to static dipole polarizability; III B, $S(-1)$, $L(-1)$, related to the total cross section for inelastic scattering; III C, $S(0)$, $L(0)$, related to the Thomas-Reiche-Kuhn sum rule and stopping power; III D, $S(1)$, related to total electronic kinetic energy, and $L(1)$, related to straggling; III E, $S(-3)$, related to nonadiabatic interaction of a charged particle with an atom; and III F, $S(-4)$ and $S(-6)$, related to the frequency-dependent refractive index and the Verdet constant.

This list is extensive but not exhaustive. For instance, by convoluting moments for two atoms, one can compute the van der Waals C_6 coefficient from our data.[16-18] We do not include such applications in the scope of this work. Otherwise, parameters not discussed explicitly, such as

TABLE I. Moments $S(\mu)$, $-6 \leq \mu \leq 1$. The format $A \pm n$ means $A \times 10^{\pm n}$.

Z	$S(-6)$	$S(-5)$	$S(-4)$	$S(-3)$	$S(-2)$	$S(-1)$	$S(0)$	$S(1)$
2	5.049−2	8.097−2	1.332−1	2.273−1	4.112−1	8.221−1	1.999	7.709
3	8.904+4	1.274+4	1.824+3	2.614+2	3.772+1	5.865	3.000	2.122+1
4	4.112+3	1.081+3	2.842+2	7.490+1	1.993+1	5.671	4.000	4.089+1
5	3.741+2	1.342+2	5.098+1	2.052+1	8.844	4.399	4.999	6.734+1
6	3.826+1	2.012+1	1.121+1	6.687	4.394	3.498	5.999	1.012+2
7	5.888	4.208	3.202	2.644	2.468	2.900	7.000	1.430+2
8	1.216	1.121	1.108	1.205	1.519	2.482	8.001	1.936+2
9	3.166−1	3.617−1	4.459−1	6.142−1	1.003	2.175	9.003	2.539+2
10	9.751−2	1.343−1	2.008−1	3.408−1	6.990−1	1.940	1.000+1	3.160+2
11	7.304+4	1.124+4	1.730+3	2.665+2	4.132+1	7.584	1.100+1	3.950+2
12	8.726+3	2.131+3	5.209+2	1.275+2	3.139+1	8.619	1.200+1	4.824+2
13	8.374+3	1.685+3	3.716+2	9.165+1	2.555+1	8.673	1.300+1	5.808+2
14	8.250+2	2.745+2	9.778+1	3.759+1	1.570+1	7.706	1.400+1	6.799+2
15	1.314+2	6.362+1	3.252+1	1.763+1	1.022+1	6.853	1.502+1	7.986+2
16	2.938+1	1.903+1	1.292+1	9.233	7.011	6.127	1.601+1	9.289+2
17	8.220	6.776	5.836	5.275	5.055	5.559	1.701+1	1.072+3
18	2.664	2.706	2.872	3.196	3.768	5.086	1.802+1	1.259+3

TABLE II. Moments $L(\mu)$, $-6 \leq \mu \leq 1$. The format $A \pm n$ means $A \times 10^{\pm n}$.

Z	$L(-6)$	$L(-5)$	$L(-4)$	$L(-3)$	$L(-2)$	$L(-1)$	$L(0)$	$L(1)$
2	2.335−2	3.915−2	6.841−2	1.271−1	2.603−1	6.304−1	2.097	1.367+1
3	−1.731+5	−2.477+4	−3.544+3	−5.740+2	−7.265−1	−9.920	2.749	5.610+1
4	−5.497+3	−1.444+3	−3.794+2	−9.969+1	−2.614+1	−6.392	4.173	1.297+2
5	−3.944+2	−1.337+2	−4.789+1	−1.805+1	−7.031	−2.346	6.407	2.404+2
6	−2.564+1	−1.238+1	−6.199	−3.179	−1.546	−1.412−1	9.101	3.937+2
7	−2.138	−1.292	−7.578−1	−3.701−1	4.330−2	1.050	1.212+1	5.945+2
8	−1.334−1	−5.617−2	3.336−2	1.761−1	5.064−1	1.733	1.542+1	8.505+2
9	3.266−2	6.030−2	1.148−1	2.412−1	6.083−1	2.142	1.896+1	1.169+3
10	2.815−2	4.775−2	9.164−2	2.076−1	5.917−1	2.394	2.267+1	1.488+3
11	−1.367+5	−2.103+4	−3.237+3	−4.982+2	−7.639+1	−9.648	2.427+1	1.930+3
12	−1.230+4	−3.004+3	−7.337+2	−1.793+2	−4.364+1	−8.825	2.625+1	2.433+3
13	−1.374+4	−2.631+3	−5.419+2	−1.228+2	−3.095+1	−7.090	2.876+1	3.015+3
14	−9.331+2	−2.932+2	−9.731+1	−3.444+1	−1.294+1	−3.708	3.176+1	3.591+3
15	−9.863+1	−4.447+1	−2.089+1	−1.025+1	−5.147	−1.285	3.509+1	4.322+3
16	−1.340+1	−7.830	−4.683	−2.848	−1.651	4.079−1	3.863+1	5.143+3
17	−1.758	−1.165	−7.354−1	−3.938−1	−1.709−2	1.599	4.232+1	6.062+3
18	−1.326−2	1.000−1	2.370−1	4.252−1	7.665−1	2.467	4.622+1	7.370+3

$L(-2)$, are not known to be related to physical quantities.

A. $S(-2)$

The quantity $S(-2)$ is directly proportional to the static dipole polarizability α, i.e., $S(-2) = \alpha/4a_0^3$. Figure 1 shows the variation of $S(-2)$ with atomic number, together with the contribution due only to $S_D(-2)$, which denotes valence excitation or discrete excitation from the outermost subshell. A two-order-of-magnitude variation in each row of the Periodic Table is apparent. The lowest values correspond to the compact, "hard," rare-gas atoms, and the largest values to the diffuse easily polarizable alkali-metal atoms. $S(-2)$ is completely dominated by the contribution from the outer shell. For the alkali metals and alkaline earths, nearly all of the contribution comes from the valence excitations of the outer s subshell. For boron and aluminum, $S_D(-2)$ (now confined by definition to the singly occupied p subshell) decreases. The nonvalence part, $S_A(-2)$, is due to discrete, autoionizing excitations of the outer s subshell. From these Group-III atoms to the rare gases, both the valence excitation and nonvalence excitation contributions decrease as the atom shrinks and becomes less polarizable. Hence, although the total oscillator strength increases, $S(-2)$ decreases as the oscillator-strength distribution shifts to higher excitation energy. Two general remarks follow from Fig. 1. First, $S(-2)$ is very similar for atoms in the same column of the Periodic Table. This is to be expected since only the valence shell is important and its properties repeat in successive rows of the Periodic Table. From this we can predict that similar variations will be found throughout the periodic system when s or p subshells are filling. Second, the same qualitative behavior can be expected for $S(\mu)$ with $\mu<-2$ since these moments also depend exclusively on low-energy excitations. This is observed in Table I.

The theoretical and experimental determination

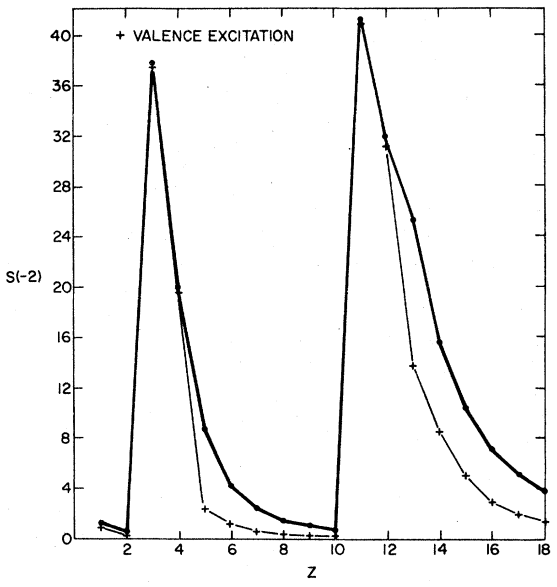

Fig. 1. Moment $S(-2)$ of the oscillator-strength distribution based on the Herman-Skillmann model, plotted as a function of atomic number Z. The contribution from the discrete excitations of the valence subshell is shown by the light line with crosses, the total $S(-2)$ being represented by the solid line with dots.

of static dipole polarizabilities is the subject of a vast literature. The most recent and extensive compilation in this field is by Teachout and Pack.[19] Figure 2 compares our results with values of $S(-2)$ determined from polarizabilities recommended by Teachout and Pack,[19] and from those calculated by Stevens and Billingsley[20] from coupled-multiconfigurational self-consistent-field (CMCSCF) wave functions stated to give polarizabilities accurate to within 5%. We consider the agreement with experiment and more accurate calculations to be good and the systematics exhibited by our calculations reliable.

In Table III we compare our results with the calculation by Stevens and Billingsley[20] and with a selected subset[21-30] of results from Teachout and Pack. We have chosen to compare five classes of values: (a) The present calculation, which is equivalent to first-order perturbation calculations in a Hartree-Slater basis. Effect of higher-order perturbations are discussed by Hameed.[31] (b) The approximate uncoupled Hartree-Fock results, denoted by SCF (as in Ref. 19) in Table III. We include these quantities in our comparison because, owing to the comparative ease of computation, they are available for all atoms in the Periodic Table. (c) Coupled Hartree-Fock (CHF) results. These calculations have been done in relatively few cases (in all, for six atoms in the first two rows). (d) So-called "accurate" results. The CMCSCF results of Stevens and Billingsley for the atoms Li through Ne which are very refined calculations including effects of configuration mixing. The variation-perturbation results[23] on He are of comparable quality. Comparison of these results with CHF results represent the importance of configuration mixing for $S(-2)$ evaluation. (e) Experimental results. The "preferred" experimental data from Teachout and Pack are listed for comparison.

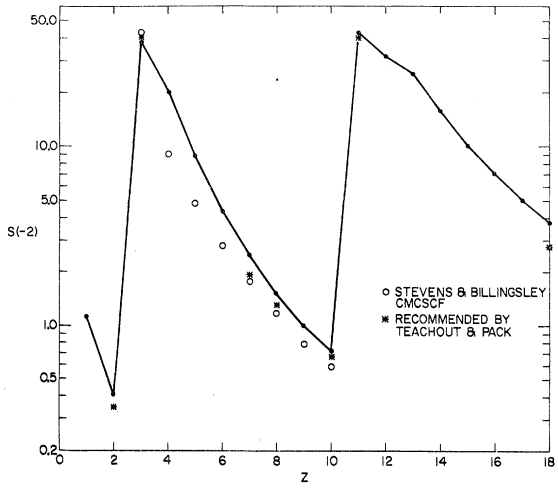

Fig. 2. Values of $S(-2)$ selected from various sources, plotted as a function of atomic number Z. The results of the present work are denoted by solid dots, connected by a solid line. Open circles represent CMCSCF results from Ref. 20; "best" values, adopted by Teachout and Pack (Ref. 19) are represented by asterisks.

The data in Table III show that the Hartree-Slater results are systematically larger than those from the other souces listed. The only exception is for Li, where the HS value is larger than the experimental and SCF values, but smaller than the CHF and CMCSCF results. Therefore, the HS "atoms" are less stable when acted on by a perturbing electric field than those from the other theoretical models. Comparison of HS and SCF values indicates that the latter tend to be more accurate except for the alkali metals. The general superiority of the SCF values may be attributed to the proper treatment of exchange in computing the SCF wave functions. For the CHF treatment, the agreement with experiment is best for the alkali metals and rare gases. The deviations are largest for the alkaline earths, and decrease steadily as the valence p shell fills. This observation is explained by the comparison of CHF and CMCSCF calculations, which indicate the importance of configuration interaction for the evaluation of $S(-2)$. This effect is largest for Be and Mg, in which the np^2 configuration strongly admixes with the valence ns^2 configuration. For succeeding atoms with increasingly filled np orbitals, the difference between CMCSCF and CHF values diminishes.

B. $S(-1)$ and $L(-1)$

The total cross section σ_{tot} for inelastic scattering of fast charged particles by an atom[32] is governed primarily by $S(-1)$, and also depends on $L(-1)$ as well as on certain nondipole properties. Because we have fully reported elsewhere[33] the evaluation of σ_{tot} for all atoms up to Ar, we shall present below only a few additional remarks on $S(-1)$ and $L(-1)$ themselves.

The sum rule

$$S(-1) = \sum_{i=1}^{Z} \sum_{j=1}^{Z} \frac{\langle x_i x_j \rangle}{a_0^2} \tag{8}$$

is well known,[1,2] where $\langle\ \rangle$ denotes the ground-state expectation value, x_i a Cartesian-coordinate component of the ith atomic electron, and a_0 the Bohr radius. Therefore, $S(-1)$ is roughly the squared radius $\sum_i \langle x_i^2 \rangle$ of the atom, modified by correlation terms $\langle x_i x_j \rangle_{i \neq j}$. The quantity $\sum_i \langle x_i^2 \rangle$ is proportional to the diamagnetic susceptibility, and its value has been computed within nonrela-

TABLE III. Comparison of $S(-2)$ values.

Atom	$S(-2)$	α (Å^3)	Source
He	0.411	0.244	Present
	0.371	0.220	SCF [a]
	0.3307	0.1960	Coupled HF [b]
	0.345 792	0.204 956	Accurate [c]
	0.3489 ± 0.0003	0.2068 ± 0.0002	Experiment [d]
Li	37.7	22.3	Present
	27.0	16.0	SCF [a]
	42.5	25.2	Coupled HF [b]
	42.80	25.37	Accurate [e]
	37 ± 3	22 ± 2	Experiment [f]
Be	19.9	11.8	Present
	13.1	7.77	SCF [a]
	11.4	6.76	Coupled HF [b]
	9.13	5.41	Accurate [e]
	$9.04 < S(-2) < 11.2$	$5.36 < \alpha < 6.62$	Experiment [g]
B	8.84	5.24	Present
	5.79	3.43	SCF [a]
(^2P state)	4.81	2.85	Accurate [e]
C	4.39	2.60	Present
	2.95	1.75	SCF [a]
(^1S state)	2.99	1.77	
(^1D state)	2.85	1.69	Accurate [e]
(^3P state)	2.80	1.66	
N	2.47	1.46	Present
	1.75	1.04	SCF [a]
(^4S state)	1.70	1.01	
(^2D state)	1.81	1.07	Accurate [e]
(^2P state)	1.77	1.05	
	1.91 ± 0.10	1.13 ± 0.06	Experiment [h]
O	1.52	0.901	Present
	1.23	0.732	SCF [a]
(^1S state)	1.20	0.71	
(^1D state)	1.18	0.70	Accurate [e]
(^3P state)	1.16	0.69	
	1.30 ± 0.10	0.77 ± 0.06	Experiment [h]
F	1.00	0.593	Present
	0.903	0.535	SCF [a]
(^2P state)	0.79	0.47	Accurate [e]
Ne	0.699	0.414	Present
	0.666	0.395	SCF [a]
	0.5895	0.3494	Coupled HF [i]
	0.592	0.351	Accurate [e]
	0.666	0.395	Experiment [j]
Na	41.3	24.5	Present
	31.4	18.6	SCF [a]
	$40.8 < S(-2) < 41.2$	$24.2 < \alpha < 24.4$	Experiment [g]
Mg	31.4	18.6	Present
	23.8	14.1	SCF [a]
	20.31	12.04	Coupled HF [i]
	$11.8 \pm 3 < S(-2) < 12.5 \pm 3$	$7.0 \pm 1.8 < \alpha < 7.4 \pm 1.8$	Experiment [k,l]
Al	25.6	15.2	Present
	18.6	11.0	SCF [a]
Si	15.7	9.31	Present
	11.5	6.81	SCF [a]
P	10.2	6.05	Present
	7.46	4.42	SCF [a]
S	7.01	4.15	Present
	5.82	3.45	SCF [a]
Cl	5.06	3.00	Present
	4.40	2.61	SCF [a]
Ar	3.77	2.23	Present
	3.36	1.99	SCF [a]
	2.649	1.570	Coupled HF [i]
	2.770	1.642	Experiment [j]

[a] Approximate uncoupled Hartree-Fock calculations in Ref. 21.
[b] Coupled Hartree-Fock calculations in Ref. 22.
[c] Perturbation-variation method in Ref. 23.
[d] Dielectric-constant measurements in Ref. 24.
[e] Multiconfigurational SCF calculations in Ref. 20.
[f] Atomic-beam deflection measurements in Ref. 25.
[g] Analysis of oscillator-strength sums in Ref. 26.
[h] Analysis of optical interferometry data in Ref. 27.
[i] Coupled Hartree-Fock calculations in Ref. 28.
[j] Analysis of index of refraction data in Ref. 29.
[k] Analysis of oscillator-strength sums in Ref. 30.
[l] See *note added in proof*.

tivistic and relativistic Hartree-Fock models for every atom.[34-36]

The quantity $S(-1)$ is shown in Fig. 3, together with the contribution due to valence excitations only and the contribution due to all discrete transitions $S_D(-1)$. Consistent with Eq. (8), $S(-1)$ is the smallest for rare-gas atoms, and largest in the vicinity of the alkaline-earth elements. The local maximum in this region is expected to repeat in subsequent rows since barium is known to be the largest atom. Thus, $S(-1)$ shows the same qualitative behavior as $S(-2)$.

Differences do arise, however, because of the increased importance of higher excitation energies in Eq. (5). One difference is a net increase with Z; $S(-1)$ reflects an increase in the number of electrons, which is manifest in higher excitation energies in the oscillator-strength distribution. Another difference is seen in the contribution of nonvalence excitations. Even for the alkalis, the continuous spectrum contributes about 10%. At $Z = 5$ and 13, the valence-excitation part is small,

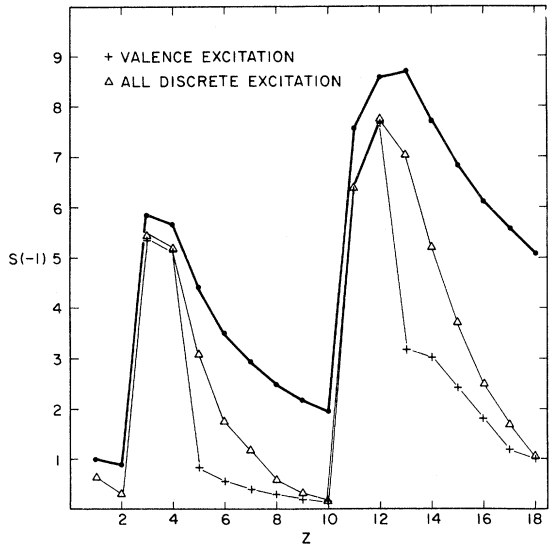

Fig. 3. Moment $S(-1)$ of the oscillator-strength distribution based on the Herman-Skillman model, plotted as a function of atomic number Z. The contribution from the discrete excitations of the valence subshell only is shown by the light line with crosses, the contribution from all discrete excitations by the light line with triangles, and the total $S(-1)$ by the solid line with dots.

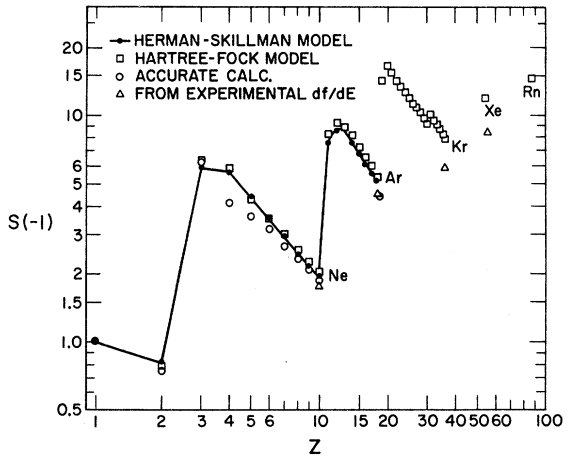

Fig. 4. Values of $S(-1)$ selected from various sources, plotted as a function of atomic number Z. Note that both horizontal and vertical scales are logarithmic. The dots connected by lines represent values from the Herman-Skillman model. The squares show results (Refs. 17, 33, 40, 41) computed as ground-state expectation values [Eq. (8)] in the Hartree-Fock model. The open circles show accurate results based on ground-state wave functions including configuration interactions (Refs. 32, 47). The triangles represent values (Ref. 37, 38, 47, 48) derived from experimental or semiempirical oscillator-strength distributions.

being comparable to the continuum part and smaller than the autoionizing part (arising from discrete excitation of the outer s subshell). As Z increases from the Group-III atoms to the rare gases, the autoionization part decreases and the continuum part increases; $S(-1)$ thus decreases less dramatically than $S(-2)$.

Figure 4 compares our Hartree-Slater results with Hartree-Fock calculations,[17,33] and experiment.[37,38] The difference between the solid circles (Hartree-Slater) and the open circles (configuration-interaction) can be attributed to correlation effects. Note that this figure includes data for $Z > 18$ and indicates the extension of the periodic structure to higher Z.

According to the Thomas-Fermi model,[39] $S(-1)$ or $\sum_i \langle x_i^2 \rangle$ should be proportional to $Z^{1/3}$; thus, the gradual increase of $S(-1)$ apart from the superimposed periodic variation is understandable. Yet the Z dependence of $S(-1)$ for rare-gas atoms is roughly $Z^{1/2}$ as opposed to the TF prediction, $Z^{1/3}$.

Clearly, any picture based on the TF model or rare-gas data could mislead an attempt to predict the value of $S(-1)$ for other atoms. The systematics seen in Fig. 4 give a much better guide, although the behavior of transition-series atoms may very well be complicated because of partially filled d shells.

Figure 5 illustrates the dependence of $L(-1)$ on Z. This curve is similar to that for $S(-1)$ but is inverted because the $\ln(E/R)$ weight factor is negative for low $E/R < 1$. Moreover, $\ln(E/R) \simeq 0$ for the range of excitation energies which embraces much of the autoionization region. Hence, $L(-1)$ depends almost entirely on valence excitations, as does $S(-2)$, and shows no over-all increase with Z.

Table IV shows comparison of our results with values selected from the literature.[2,17,32,33,37,40-53]

Understandably our $S(-1)$ values are close to HF values, because the HS model we used is an approximation to the HF model. The trend that the HS values are smaller than the HF values and thus happen to be closer to CI (configuration-interaction) or empirical values except for He and B (the latter of which is not included in Table IV) warrants no serious concern, as we have explained elsewhere.[33]

Our $S(-1)$ values agree with better values, either from CI calculations or from empirical oscillator-strength distributions, within 10% for most of the atoms we treated. For Ar, as an exception, the agreement is within 20%. Therefore, it is probably safe to say that our data are sufficiently realistic to reveal gross systematics for all other atoms for which no better are available.

Turning to our $L(-1)$ values in Table IV, we

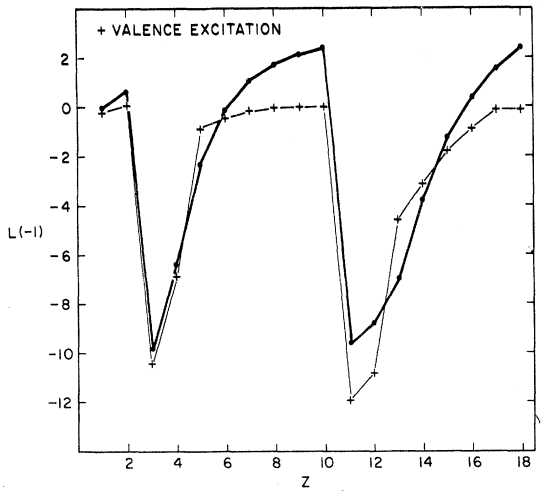

Fig. 5. Quantity $L(-1)$ for the oscillator-strength distribution based on the Herman-Skillman model, plotted as a function of atomic number Z. The light line with crosses shows the contribution from the discrete excitations of the valence subshell only, and the heavy line shows the total $L(-1)$.

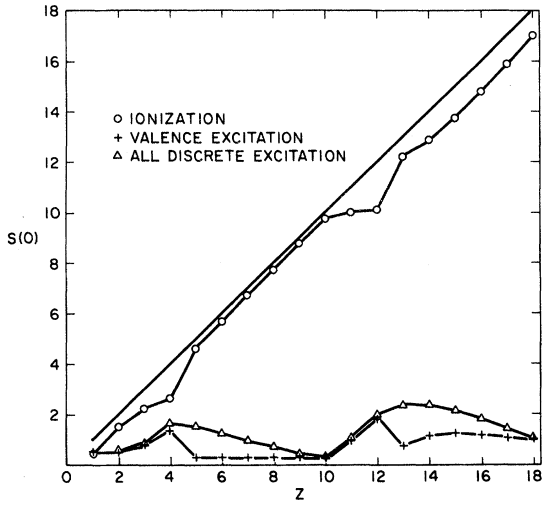

Fig. 6. Moment $S(0)$ of the oscillator-strength distribution based on the Herman-Skillman model, plotted as a function of atomic number Z. The total $S(0)$ is denoted by the solid line. Also shown are contributions from all discrete excitations (Δ), discrete excitations of the valence subshell only (+), and ionization (○).

find that they agree even better with accurate values than our $S(-1)$ values do. Hence, our $L(-1)$ values for other atoms should be reasonably reliable. Our $L(-1)$ value 2.47 for Ar agrees fairly well with the empirical value of 2.85, but is strongly incompatible with the moment-theory bounds given by Langhoff and Yates.[44] We attribute the discrepancy to the use of an inaccurate $S(-1)$ value 5.3 in the moment-theory analysis; although the moment theory is mathematically sound, it can yield misleading results unless input data are highly accurate.

C. $S(0)$ and $L(0)$

The sum $S(0)$ is shown in Fig. 6, together with ionization, valence excitation, and total discrete contributions. The breakdown of $S(0)$ is interesting since it is an unweighted sum of the oscillator strength and indicates directly the contributions of ionization and discrete excitations to the oscillator strength. Figure 6 shows that the ionization part increases linearly with Z and represents the bulk of the oscillator strength. Of the remaining part, the valence excitation is significant for the alkali metals and alkaline earths and autoionizing transitions are significant when the p shell begins to fill.

Figure 7 shows the shellwise contributions. Here all subshells contribute roughly in proportion to this occupation number Z_{nl}. However, this is not strictly adhered to, and the $s \rightarrow p$ and $p \rightarrow s$ channels exchange oscillator strength among them-

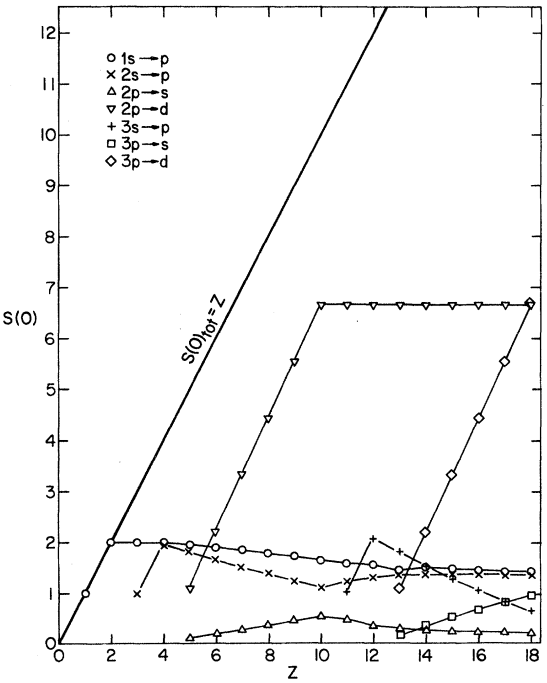

Fig. 7. Contributions from individual subshells to the moment $S(0)$, plotted as a function of atomic number Z. Because the $2p \rightarrow d$ contribution is $\frac{10}{3}$ per $2p$ electron according to Eq. (4.22) of Ref. 2, the horizontal line for $Z \geq 10$ lies at $\frac{20}{3} = 6.67$. The excess of this value above 6 is exactly compensated by the (negative) $2p \rightarrow s$ contribution inclusive of the $2p \rightarrow 1s$ and $2p \rightarrow 2s$ transitions.

TABLE IV. Comparison of values of $S(-1)$ and $L(-1)$ selected from various sources.

Atom	$S(-1)$	Sources	$L(-1)$	Sources
He	0.822	Present work	0.6304	Present work
	0.7899	HF [a,b]		
	0.7525	Accurate [c]	0.6382	Semiempirical OSD [d,e]
			0.646 ± 0.0015	Moment theory [f]
			0.647 ± 0.007	Moment theory [g]
Li	5.865	Present work	−9.920	Present work
	6.189	HF [a]		
	6.037	CI [a]		
	5.97	Semiempirical OSD [d,h]		
	6.085	Variation-perturbation theory [i]		
Ne	1.941	Present work	2.394	Present work
	2.023	HF [j]		
	2.027	HF [k]		
	1.881	CI [l]		
	1.885	Semiempirical OSD [d,l]	2.360	Semiempirical OSD [d,l]
	1.924	CI [k]	2.431	Semiempirical OSD [d,k]
	1.95	Adopted value [m]	2.49 ± 0.08	Moment theory [f]
			2.48 ± 0.22	Moment theory [g]
	1.897	Semiempirical OSD [d,n]		
	1.96	Semiempirical OSD [d,o]		
	1.94	Semiempirical OSD [d,h]		
	1.922	Theoretical OSD [p]		
			2.35 ± 0.24	Variation-perturbation theory [q]
Mg	8.619	Present work	−8.825	Present work
	9.18	HF [r]		
	9.194	HF [k]		
	9.19	HF [a]		
Ar	5.086	Present work	2.47	Present work
	5.502	HF [j]		
	5.474	HF [a]		
	5.455	HF [r]		
	4.437	Semiempirical OSD [d,n]		
	5.3	Adopted value [m]	4.34 ± 0.74	Moment theory [g]
	4.268	CI [k]	2.85	Semiempirical OSD [d,k]
	4.409	Semiempirical OSD [d,s]	2.843	Semiempirical OSD [d,k]

[a] References 33 and 17; the Hartree-Fock results given in these two references are the same within a few tenths of a percent for every atom He through Ar.
[b] Reference 41.
[c] Reference 42.
[d] The acronym "OSD" stands for oscillator-strength distribution.
[e] Reference 32.
[f] Reference 43.
[g] Reference 44.
[h] Reference 45.
[i] Reference 46.
[j] Reference 40.
[k] Reference 47.
[l] Reference 48.
[m] Reference 2, Table II.
[n] Reference 49.
[o] Reference 50.
[p] Reference 51.
[q] Reference 52.
[r] Reference 53.
[s] Reference 37.

selves. The $p \rightarrow d$ channels, on the other hand, behave hydrogenically since there are no bound d orbitals and the $l = 2$ wave functions are largely governed by a nearly hydrogenic field outside the ion core. During the transition-metal series, these partial cross sections will also exchange strength with the other subshells and will no longer appear perfectly linear.

The stopping power for fast charged particles depends on $L(0)$. Indeed, $L(0)$ is the only nontrivial target property contained in the Bethe asymptotic formula.[54,55] In this context, one traditionally discusses the mean excitation energy I_0 defined by

$$\ln(I_0/R) \equiv L(0)/S(0) = L(0)/Z. \tag{9}$$

The contributions to $L(0)$ from different shells are seen in Fig. 8. First of all, notice that the ordinate there represents the ratio $L(0)/Z$. The contributions from every subshell to $L(0)$ itself increases with Z—a consequence of the universal displacement of subshell oscillator strengths to higher E owing to tighter and tighter binding. For the lightest atoms ($Z \leq 6$), the $1s \rightarrow p$ transition dominates. For succeeding atoms, the $1s \rightarrow p$ transition becomes relatively less important,

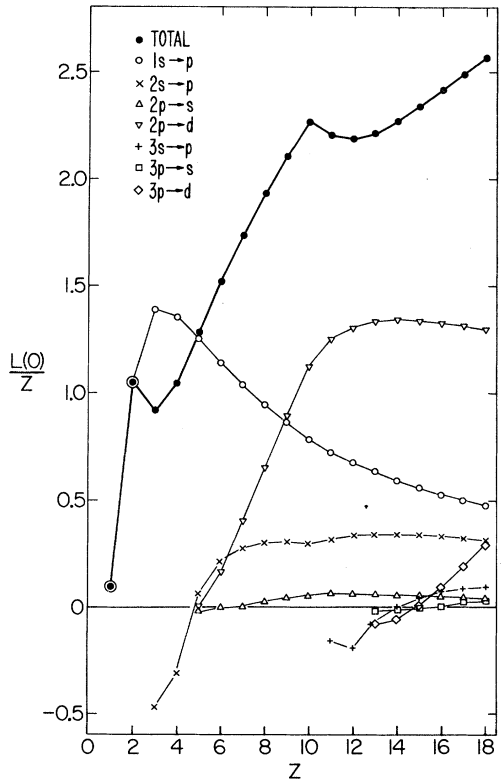

Fig. 8. Shellwise contributions to the quantity $L(0)/Z$ plotted as a function of atomic number Z. The meaning of the different symbols is shown in the insert.

while $2p \rightarrow d$ and $2s \rightarrow p$ contributions rapidly grow with the filling of the L shell but eventually flatten out. The $2p \rightarrow s$ transition contributes to $L(0)$ only modestly, because its oscillator strength is much smaller than the $2p \rightarrow d$ strength (as seen in Fig. 7) and is chiefly distributed at E near R, for which $\ln(E/R) \simeq 0$.

For the second-row atoms, the $1s \rightarrow p$ contributions remain substantial, but keep declining. The $2p \rightarrow d$ contributions are now flat, but still amount to over 50% of the total $L(0)/Z$. A remarkable contrast to the second-row atoms to the first-row atoms is that the $3s \rightarrow p$, $3p \rightarrow d$, and $3p \rightarrow s$ contributions are fairly small and comparable among themselves. This observation means that much of the oscillator strength of the M electrons reside at fairly low excitation energies at which $\ln(E/R)$ is inappreciable.

The relative importance of the different shell contributions seen in Fig. 8 serves as a general guide for accurate evaluation of $L(0)$, say, from empirical (or otherwise accurate) oscillator-strength distributions of various atoms and molecules. For instance, the role of the $1s \rightarrow p$ transition is invariably appreciable for any molecule composed of atoms in the first two rows, despite the relatively small number of K electrons. This is so because the K-shell oscillator strength is concentrated at high E.

It is apparent from the above discussion that I_0 defined by Eq. (9) is roughly proportional to Z, as Bloch[56] pointed out on the basis of the Thomas-Fermi model. Therefore, it is appropriate to consider the ratio I_0/Z as a function of Z, as shown in Fig. 9. There we see a periodic variation mainly due to the valence-shell structure, whereas the approximate constancy of I_0/Z (except for H and He) reflects the important role of inner-shell excitations.

Table V shows comparison of our results with earlier data selected from the literature.[37,40,41,44,46,48,52,57-68] Theoretically, $L(0)$ or I_0 has been evaluated (a) directly from a computed or semiempirical oscillator-strength distribution,[37,48,57,58,63,66] (b) via a variation-perturbation theory, or (c) through a fitting[40,41,43,44,61,62] of $S(\mu)$ data by use of the relation

$$L(0) = \frac{dS(\mu)}{d(\mu)}\bigg|_{\mu=0}.$$

Our values of I_0/Z agree reasonably well with accurate theoretical values obtained by methods (a) and (b) for rare gases and for Li, and appear in harmony with values from the $S(\mu)$ fitting [method (c)], except for a few instances. One exception is Be, where our value $I_0 = 38.6$ eV is

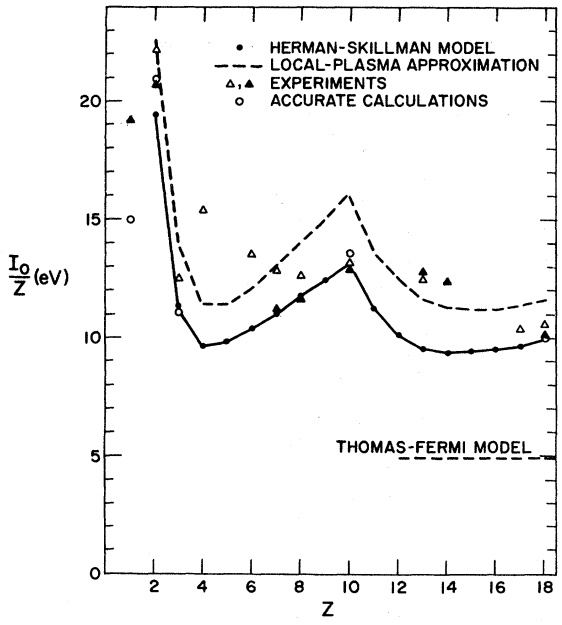

Fig. 9. Mean excitation energy I_0 for stopping power. The vertical axis represents the ratio I_0/Z measured in eV, and the horizontal axis the atomic number Z. The line with dots shows present results from the oscillator-strength distribution based on the Herman-Skillman model. The open circles show accurate values derived from semiempirical oscillator-strength distributions or from theory. The triangles are values derived from stopping-power measurements. The open triangles show data by Turner and co-workers (Ref. 64), the filled triangles those by Bichsel and co-workers (Refs. 65, 67, 68). The dot-dashed line represents values from the local-plasma model (Ref. 70). The horizontal dashed line represents the result of the Thomas-Fermi model (Ref. 13).

much lower than the 66.1 eV of Dalgarno,[61] who fitted Hartree-Fock values of $S(\mu)$ for $\mu = 2$, 1, -1, and $S(-2)$ from an experimental polarizability to an analytic expression. For Be, the importance of electron-correlation effects, missing from our model, is well known.[69] Since our $S(-1)$ value is close to the HF value, apparently Dalgarno's use of the experimental $S(-2)$ is crucial for the better I_0 value. However, the situation remains unsettled, since the experimental I_0 of Table V is derived from solid-state measurements.

Attention may be drawn to some discrepancies from the values of McGuire,[63] who started with the same Herman-Skillman[3] potential $V(r)$ to compute df/dE and thence I_0. He introduced a piecewise linear approximation to $rV(r)$ to facilitate wave-function calculations, while we have accurately solved the radial Schrödinger equation with the numerically tabulated $V(r)$. Thus, his results should have been in complete agreement with ours, if his mathematical approximation were totally adequate.[14] Actually, his values of I_0/Z are seriously discordant with ours for $Z \geq 8$, and exhibit a maximum for F rather than for Ne—a trend that is hard to explain from physics.

Chu and Powers[70] used the local-plasma model of Lindhard and Scharff,[71] who had suggested setting

$$\ln I_0 = Z^{-1} \int \ln[\gamma \hbar \omega_p(r)]\, \rho(r) 4\pi r^2\, dr, \tag{10}$$

where γ is a constant and $\omega_p(r)$ is the plasma frequency

$$\omega_p(r) = [4\pi e^2 \rho(r)/m]^{1/2} \tag{11}$$

TABLE V. Comparison of $L(0)$ and I_0 values selected from various sources.

Atom	$L(0)$	I_0 (eV)	I_0/Z (eV)	Source
He	2.097	38.82	19.41	Present work
	2.245	41.8	20.9	Semiempirical OSD [a,b]
	2.268	42.48	21.14	Semiempirical OSD [a,c]
	2.254	42.0	21.0	Variation-perturbation theory [d]
	2.26	42.1	21.1	Variation-perturbation theory [e]
	2.240	41.7	20.85	$S(\mu)$ fit [f]
	2.11	39	19.5	$S(\mu)$ fit [g]
	2.26	42.19	21.1	$S(\mu)$ fit [h]
	2.26 ± 0.015	42.0 ± 0.36	21.0 ± 0.18	Moment theory [i]
	2.28 ± 0.03	42.1 ± 1.3	21.05 ± 0.65	Moment theory [j]
	2.196	40.8	20.4	Theoretical OSD [a,k]
	2.361	44.3	22.15	Experimental [l]
	2.223	41.35	20.68	Experimental [m]
Li	2.749	34.02	11.34	Present work
	2.68	33	11	Variation-perturbation theory [n]
	3.14	38.8	12.9	$S(\mu)$ fit [f]
	2.66 ± 0.30	33 ± 3.5	11 ± 1	$S(\mu)$ fit [h]
	2.765	34.2	11.4	Theoretical OSD [a,k]
	3.03	37.4	12.5	Experimental [l]

TABLE V. (continued)

Atom	L (0)	I_0(eV)	I_0/Z (eV)	Source
Be	4.173	38.62	9.65	Present work
	6.323	66.1	16.5	$S(\mu)$ fit [f]
	4.167	38.6	9.64	Theoretical OSD [a,k]
	6.047	61.7	15.4	Experimental [l]
B	6.407	49.00	9.80	Present work
	6.457	49.5	9.90	Theoretical OSD [a,k]
C	9.101	62.01	10.33	Present work
	9.253	63.6	10.6	Theoretical OSD [a,k]
	10.73	81.3	13.55	Experimental [l]
N	12.125	76.91	10.99	Present work
	12.13	77.0	11.0	Theoretical OSD [a,k]
	12.58	82.1	11.7	Empirical OSD [o] of N_2
	13.19	89.6	12.8	Experimental [l]
	12.22	78.0	11.14	Experimental [m]
O	15.42	93.50	11.69	Present work
	15.89	99.2	12.4	Theoretical OSD [a,k]
	16.04	101	12.6	Experimental [l]
	15.34	92.6	11.6	Experimental [m]
F	18.96	111.8	12.43	Present work
	19.30	116.1	12.9	Theoretical OSD [a,k]
Ne	22.67	131.3	13.1	Present work
	24.00	150	15.0	$S(\mu)$ fit [p]
	22.10	124	12.4	Theoretical OSD [a,k]
	23.06	136.5	13.65	Semiempirical OSD [a,g]
	22.2 ± 1.0	125 ± 12	12.5 ± 1.2	Variation-perturbation theory [r]
	22.03 ± 1.5	123 ± 20	12.3 ± 2.0	Moment theory [i]
	22.50 ± 2.6	129 ± 38	12.9 ± 3.8	Moment theory [j]
	22.72	132	13.2	Experimental [l]
	22.53	129.5	12.95	Experimental [m]
Na	24.27	123.6	11.23	Present work
	23.21	112	10.2	Theoretical OSD [a,k]
Al	28.755	124.3	9.56	Present work
	32.28	163	12.5	Experimental [l]
	32.60	167	12.8	Experimental [s]
Si	31.76	131.5	9.39	Present work
	35.60	173	12.4	Experimental [s]
Cl	42.32	164.0	9.65	Present work
	43.52	176	10.4	Experimental [l]
Ar	46.22	177.4	9.85	Present work
	50.10	220	12.2	$S(\mu)$ fit [p]
	37.8 ± 8.5	111 ± 61	6.2 ± 3.7	Moment theory [j]
	47.36	189	10.5	Experimental [l]
	46.68	182	10.1	Experimental [t]
	46.354	178.7	9.93	Semiempirical OSD [a,u]

[a] The acronym "OSD" stands for oscillator-strength distribution.
[b] Reference 57.
[c] Reference 58.
[d] Reference 59.
[e] Reference 60.
[f] Reference 61.
[g] Reference 41.
[h] Reference 62.
[i] Reference 43.
[j] Reference 44.
[k] Reference 63.
[l] Reference 64.
[m] Reference 65.
[n] Reference 46.
[o] Reference 66.
[p] Reference 40.
[q] Reference 48.
[r] Reference 52.
[s] Reference 67.
[t] Reference 68.
[u] Reference 37.

corresponding to the local electron density $\rho(r)$ at distance r from the nucleus. This procedure amounts to taking

$$\frac{df}{dE} = \langle \delta(E - \gamma\hbar\omega_p(r)) \rangle, \tag{12}$$

where the brackets denote the ground-state expectation value. Chu and Powers used the electron density tabulated by Herman and Skillman[3] and set $\gamma = 2^{1/2}$. This suggestion of Lindhard and Scharff is based upon intuitive arguments rather than a mathematical deduction from the standard definition [Eqs. (1) and (4)] of df/dE.

With this qualification in mind, we compare the I_0/Z values of Chu and Powers with ours and find a remarkably similar trend. Either set of data shows maxima for rare gases and minima in the middle of each row of the Periodic Table. However, the minimum in the second row is much shallower in the data by Chu and Powers. The most important difference is the absolute magnitude; the results of Chu and Powers are consistently larger than ours by 20 to 30%.

Ball, Wheeler, and Fireman[13] have recently published the dipole spectrum of the TF model, an ultimate solution to the problem posed by Bloch.[56] The TF spectrum yielded $I_0/Z = 4.95$ eV, as indicated by the dashed line on Fig. 8. Clearly, the value is too small to be realistic (even for atoms beyond Ar), and exemplifies a defect in the TF model.

Experimental values of I_0 are customarily deduced from fits of the Bethe formula (sometimes with modifications as noted below) to measured stopping powers at different charged-particle velocities. Even though the stopping power is now measured precisely and accurately in many materials, the data analysis involves considerable intricacies, as fully discussed by Turner[72] and by Bichsel.[73] For example, the fitting expression often requires an additional term commonly called inner-shell corrections,[55,72,73] which remain incompletely understood at present. Thus, different tabulations[64,72-74] of experimental I_0 sometimes present discordant values. On preparing Table V and Fig. 9, we chose as representative values the data given by Turner *et al.*[64] and by Bichsel and co-workers.[65,67,68] (In doing so, we by no means imply that the quoted values should be recommended; critical evaluation of the stopping-power data is beyond the scope of the present paper.)

An additional qualification is that the experimental I_0 values, except for those on rare gases, stem from measurements on molecules and solids, while our theoretical values pertain to free atoms. It is true that the effect of atomic aggregation upon I_0 should be accessory (as is implicit in the Bragg additivity rule[55,75]) because I_0 is largely governed by inner-shell excitations. Nevertheless, a conclusive assessment of the atomic-aggregation effect has so far been hampered by lack of realistic I_0 values for free atoms. Our data are meant to fill exactly this gap of knowledge.

For rare gases, our theoretical values are in satisfactory agreement with experimental values. The largest discrepancy from the value of Turner *et al.*[64] for He is not serious; the other experimental value[65] is virtually identical to accurate theoretical values and indicates that our value is a slight underestimate.

Our results for N and O agree excellently with the values that Hanke and Bichsel[65] deduced from measurements of N_2 and O_2. Also, our value for N is close to the value that Dalgarno *et al.*[66] calculated from a semiempirical oscillator-strength distribution for N_2. The above observation certainly supports the Bragg rule. The somewhat higher I_0 values of Turner *et al.*[64] for N and O are based on stopping powers of many chemical compounds, and probably suggest the extent of the atomic-aggregation effect.

Large discrepancies of our results for Be, C, Al, and Si from experimental values[64,68] must be attributed to the atomic-aggregation effect; indeed, the experimental values all come from measurements on solids, in which atoms are not only in a valence state but are also interacting among themselves. The above observation is in accord with discussions by Platzman[75] and by Fano.[55]

D. $S(1)$ and $L(1)$

The moment $S(1)$ can be expressed[1,2] in the alternative form

$$S(1) = \frac{4}{3R}\left\langle \frac{(\sum_j \vec{p}_j)^2}{2m} \right\rangle = \frac{4}{3R}\left[\sum_j \left\langle \frac{\vec{p}_j^{\,2}}{2m} \right\rangle + \sum_j \sum_{k \neq j} \left\langle \frac{\vec{p}_j \cdot \vec{p}_k}{2m} \right\rangle \right], \tag{13}$$

where p_j is the momentum of the jth atomic electron. The first term in square brackets is the mean kinetic energy of all the atomic electrons, which may be equated with the absolute value $|W_0|$ of the total binding energy owing to the virial theorem. For this reason we show in Fig. 10 comparison of our HS $S(1)$ values with $4|W_0|/3R$, $|W_0|$ being derived from the Thomas-Fermi (TF) model and the HF model. The $S(1)$ values lie quite close to $4|W_0|/3R$ from the HF model,[35] and therefore show that the cross term

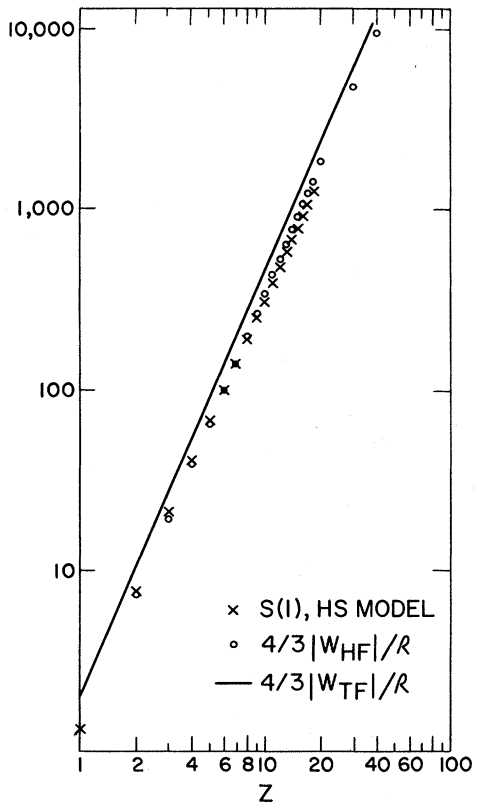

Fig. 10. Comparison of the moment $S(1)$ based on the Herman-Skillman model with approximations to $S(1)$ derived from the total energy W_{HF} from the Hartree-Fock model (Ref. 35) (circles) and the total energy W_{TF} from the Thomas-Fermi model (Ref. 39) (solid line).

$(k \neq j)$ in Eq. (13) is small. (We shall later discuss the nature of the cross term in some detail.) Our $S(1)$ values also agree rather well with the TF result[39]

$$4|W_0|/3R = 2.0507\, Z^{7/3}, \tag{14}$$

and the discrepancy from Eq. (14) may be largely attributable to the well-known inadequacy of the TF model at small r.

For $\mu \geq 0$, $S(\mu)$ shows no periodicity but rather increases monotonically as Z^n, where the value of n increases faster than μ (i.e., $n=1$ for $\mu=0$, $n \sim \frac{7}{3}$ for $\mu=1$). In the context of Eq. (5), this results from progressively weighting higher excitation energies. The periodic effect of the valence shell (low excitation energies) is therefore diminished, while the effect of inner shells is to increase $S(\mu)$ smoothly with Z, as a consequence of an increase in the inner-shell contribution to the oscillator strength.

At this point we present several remarks on the cross term

$$\Omega = \left\langle \sum_j \sum_{j \neq k} \frac{\vec{p}_j \cdot \vec{p}_k}{2m} \right\rangle \tag{15}$$

in Eq. (13), which is certainly smaller than the kinetic-energy term but is important on two counts at least. First, Ω explicitly reflects electron correlations in the ground state; note that $\Omega = 0$ in the Hartree model without exchange effects. Second, the same quantity Ω causes the specific mass-polarization effect of the nuclear motion on atomic spectra (see p. 165 of Ref. 1).

Within the HF or HS model, it is possible to show[76] that $\Omega \leq 0$ for all the atoms we treat ($Z \leq 18$). Moreover, finite contributions arise only from pairs of electrons that have the same spin and have orbital angular momenta differing by unity. We see an excellent confirmation of the above statements in the $S(1)$ values that Cummings[17] computed from the HF model according to Eq. (13). Indeed, $\Omega = 0$ for He, Li, and Be, and $\Omega < 0$ for all the succeeding atoms, which have both s and p electrons. The Ω value amounts to about -2% of the kinetic-energy term for B, steadily becomes more and more important with increasing Z, and approaches -18% for Ar, according to the HF results.[17] Our HS $S(1)$ values show qualitatively the same behavior. Yet Ω in the HS model is a little smaller in absolute magnitude than in the HF model; in the most extreme example of Ar, the HS Ω value is about -13% of the kinetic-energy term.

When one goes beyond the HF model, Ω often increases by a few percent of the kinetic energy, because of more intricate correlation effects. For instance, $\Omega > 0$ for He,[42] and for Li,[62] when it is computed from wave functions more accurate than the HF model. Also the CI value[48] of $S(1)$ for Ne is greater than the HF values, as seen in Table VI. Nevertheless, the increase due to the CI effect in Ne is too small to offset the negative sign of the HF Ω values; thus Ω remains negative in the CI calculation.[48]

Table VI presents comparison of our results with those of other workers.[2,17,37,40-45,48-50,52,62] The general agreement in all cases is good. Hence, we feel our values of $S(1)$ are uniformly in the range of 10% accuracy for all the atoms we treat. This conclusion bears out also from comparison with the HF values.[17]

The quantity $L(1)$ appears as an important parameter in the theory of straggling.[55] As in the case of $S(1)$, it is a monotonically increasing function of Z (see Table II). The discussion of the behavior of $S(1)$ can be carried over to $L(1)$ as the $\ln E$ term has only a minor effect on the gross Z dependence of $L(1)$. Again, only limited data are available for comparison. Table

TABLE VI. Comparison of values of $S(1)$ and $L(1)$.

Atom	$S(1)$	Source	$L(1)$	Source
He	7.709	Present work	13.67	Present work
	7.631	HF[a,g]	13.6	$S(\mu)$ fit[a]
	8.167	Accurate[b]	13.72	Variation-perturbation theory[c]
			13.99	OSD[d]
			14.7 ± 0.5	Moment theory[e]
			14.5 ± 1.0	Moment theory[f]
Li	21.22	Present work		
	19.82	HF[g]		
	20.74	CI[h]		
Ne	316.0	Present work	1489	Present work
	302.85	HF[i]	1356.6	$S(\mu)$ fit[i]
	330.4	OSD[j]	1518 ± 158	Moment theory[e]
	318.5	OSD[k]	1494 ± 205	Moment theory[f]
	293.7	HF[k]	1434 ± 74.2	Variation perturbation theory[n]
	321	OSD[l]	1485.2	OSD[m]
	320	Adopted[o]		
	308.80	CI[m]		
	315.3	OSD[m]		
Ar	1259	Present work	7370	Present work
	1148.6	HF[i]	6270	$S(\mu)$ fit[i]
	1150	Adopted[o]	6623 ± 1024	Moment theory[f]
	1115	OSD[p]		

[a] Reference 41.
[b] Reference 42.
[c] Reference 60.
[d] Reference 58.
[e] Reference 43.
[f] Reference 44.
[g] Reference 17.
[h] Reference 62.
[i] Reference 40.
[j] Reference 49.
[k] Reference 50.
[l] Reference 45.
[m] Reference 48.
[n] Reference 52.
[o] Reference 2.
[p] Reference 37.

VI shows that in those cases where comparison is possible, the agreement is again good.

E. $S(-3)$

The amount of electron charge displaced when an atom is put in an external uniform electric field is proportional to $S(-3)$. To see this significance, we may write the atomic wave function in the electric field ϵ (directed along the z axis) as $u_0 + \epsilon v_0$, where u_0 is the ground state. According to the first-order perturbation theory, we have

$$v_0 = \sum_{n \neq 0} E_n^{-1} (n| -e \sum_{j=1}^{Z} z_j |0) u_n, \tag{16}$$

where u_n is the nth atomic state, E_n its excitation energy measured from the ground state, and $(n| -e\sum_{j=1}^{Z} z_j |0)$ is the dipole matrix element. The summation $\sum_n$ included integration over continua. Noting the orthonormality of u_n and the definition of f_n, we calculate the norm of v_0 as

$$\int |v_0|^2 d\vec{r}_1 \cdots d\vec{r}_Z = e^2 \sum_n E_n^{-2} \left| (n| \sum_{j=1}^{Z} z_j |0) \right|^2 = 4(a_0^2/e)^2 S(-3), \tag{17}$$

where a_0 is the Bohr radius. Notice that e/a_0^2 is the atomic unit for ϵ. Because $S(-2)$ is proportional to the dipole moment induced by ϵ, the ratio $S(-2)/S(-3)$ measures the mean distance of charge displacement.

Understandably, $S(-3)$ appears in the asymptotic nonadiabatic potential for the interaction of an atom with a charged particle.[77,78]

Table VII compares $S(-3)$ values with some data selected from the literature.[17,46,48,53,78] Our values agree fairly well with presumably more accurate values for Li, Ne, and Na, but only moderately well for He. The discrepancy for Ar is serious, and shows the inadequacy of the Hartree-Slater model for describing the lowest part of the discrete spectrum, as seen also in the $S(-2)$ value (Table III). Yet, our $S(-3)$ values for other atoms in Table I should serve as a guide for estimates until better values become

TABLE VII. Comparison of $S(-3)$ values selected from the literature.

Atom	$S(-3)$	Source
He	0.227	Present work
	0.177	Recommended [a] in Ref. 78
	0.192	Uncoupled HF [b]
	0.179	Uncoupled HF [c]
	0.164	Coupled HF [b]
	0.156	Coupled HF [d]
Li	261.4	Present work
	295	Recommended in Ref. 78; variation-perturbation theory [e]
	134.1	Uncoupled HF [c]
Ne	0.340	Present work
	0.318	Recommended in Ref.78
	0.316	Semiempirical OSD [f]
	0.266	Uncoupled HF [c]
	0.239	Coupled HF [d]
Na	266.5	Present work
	275	Recommended in Ref. 78; semiempirical
	155.7	Uncoupled HF [c]
Mg	127.5	Present work
	75.7	Uncoupled HF [c]
	52.8	Coupled HF [d]
Ar	3.20	Present work
	2.08	Recommended in Ref. 78; semiempirical
	2.47	Uncoupled HF [c]
	1.66	Coupled HF [d]

[a] The quantity β_1 of Ref. 78 is equal to $4a_0^4 S(-3)$.
[b] Reference 78.
[c] Reference 17.
[d] Reference 53.
[e] Reference 46.
[f] Reference 48.

available.

Table VII also includes representative results of uncoupled HF[17] and coupled HF[53] calculations. Here we observe a continuation of the trend for $S(-2)$ seen in Table III. Namely, the HS values are consistently larger than the HF values because the HS model predicts larger f values for low-lying discrete excitations, especially the resonance transition. The HS values are close to the HF values for the "tight" atoms (i.e., rare gases), but differ for the "loose" atoms (e.g., Li, Na, and Mg) by about a factor of 2. As in the case of $S(-2)$, the HS values are closer to recommended values than the HF results except for Ar, even though the HS model is an approximation to the HF model. The situation for Mg remains particularly ambiguous owing to the lack of a recommended value.

F. $S(-4)$ and $S(-6)$

The moments $S(-4)$ and $S(-6)$ govern the frequency-dependent polarizability and thereby characterize optical dispersion properties such as the refractive index and the Verdet coefficient.[2]

Table VIII shows a comparison of our values of $S(-4)$ and $S(-6)$ with some of the literature values.[16,37,46,48,50,57,58,79,80] Our values for He, Li, Ne, and Na agree moderately well with presumably better values. The modest agreement indicates once again that the HS model gives an oscillator-strength distribution only fairly reliable for low excitation energies, which predominantly contribute to $S(-4)$ and $S(-6)$. The discrepancy of our values from better values is most serious for Ar, where electron-correlation effects both in the ground state and in any excited states are substantial, chiefly owing to the unfilled $3d$ orbitals.

IV. CONCLUDING REMARKS

The data of $S(\mu)$ and $L(\mu)$ we have presented enable one to consider systematics of the dipole spectrum of atoms from various points of view. As an epilogue we point out another angle from which the systematics may readily be seen.

Figure 11 shows plots of $\log_{10} S(\mu)$ as a function of μ for different atoms. The general behavior of $S(\mu)$ naturally classifies atoms into three groups. The first group of tight atoms (i.e., rare gases) has $S(\mu)$ that monotonically increases

TABLE VIII. Comparison of $S(-4)$ and $S(-6)$ with values selected from the literature.

Atom	$S(-4)$	$S(-6)$	Sources
He	0.133	0.0505	Present work
	0.0982	0.0321	OSD [a]
	0.0976	0.0323	OSD [b]
	0.0967	0.0320	OSD [c]
	0.0962	0.0319	Dispersion data [d]
	0.0969	0.0323	Dispersion data [e]
	0.0966	0.0319	Dispersion data [f]
Li	1824	8.90×10^4	Present work
	2137		Variation-perturbation theory [g]
	2204	1.19×10^5	Dispersion data [e]
Ne	0.2008	0.097 51	Present work
	0.1798	0.077 88	OSD [b]
	0.1815	0.079 66	Dispersion data [d]
	0.179	0.0888	Dispersion data [e]
	0.187	0.084	Dispersion data [f]
	0.1785	0.0766	OSD [h]
Na	1730	7.30×10^4	Present work
	1709	7.14×10^4	Dispersion data [e]
Ar	2.872	2.664	Present work
	1.681	1.349	OSD [b]
	1.746	1.571	Dispersion data [d]
	1.760	1.512	Dispersion data [e]
	1.749	1.475	Dispersion data [f]
	1.720	1.444	OSD [i]

[a] Reference 57.
[b] Reference 49.
[c] Reference 58.
[d] Reference 16.
[e] Reference 79.
[f] Reference 80.
[g] Reference 46.
[h] Reference 48.
[i] Reference 37.

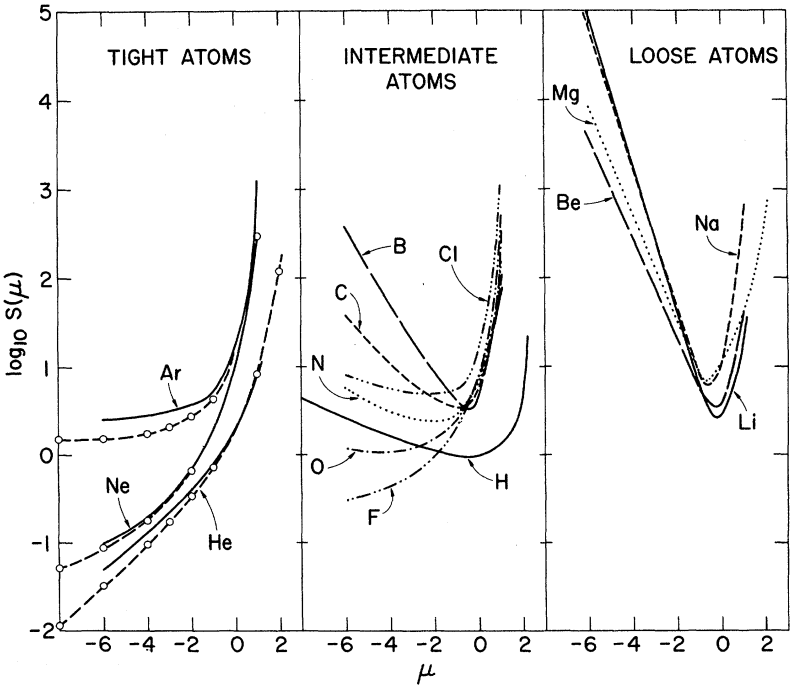

FIG. 11. Moment $S(\mu)$ for each atom as a function of μ. Note that the vertical scale is logarithmic. The open circles connected by broken lines show semi-empirical or otherwise better values for He, Ne, and Ar. The curve for H is rigorous. All the other curves are based upon the oscillator-strength distribution for the Herman-Skillman model.

with μ, a behavior that illustrates heavy concentration of the oscillator strength at higher excitation energies. The second group of loose atoms (i.e., alkalis and alkaline earths) by contrast, has $S(\mu)$ characterized by a prominent minimum near $\mu=-1$. Notice that the curve of $\log_{10}S(\mu)$ to the left-hand side of the minimum is nearly linear in μ. This behavior shows the dominance of the strong resonance excitation in those atoms. [If the oscillator-strength distribution had a single peak at an energy E_0, then we would have $S(\mu)=Z(E_0/R)^{\mu}$, in other words, $\log_{10}S(\mu)$ linear in μ.] The third group of atoms in the middle of the Periodic Table exhibits an intermediate trend in part similar to the loose atoms and in part similar to the tight atoms. Going through the first row, we observe a gradual change of the curves; first B behaves similarly to Be, succeeding atoms C, N, and O depart farther and farther from the loose-atom behavior, and finally F looks not much different from Ne. The second-row atoms have qualitatively the same trend, but the variation within the second row is limited to a much narrower range. For this reason we have omitted second-row atoms except for Cl, which shows a behavior resembling Ar. In Fig. 11 we have put H in the group of intermediate atoms for no profound reason; actually, the curve for H makes a class of its own.

Common to all atoms is the rapid increase of $S(\mu)$ for $\mu>0$. This general behavior is understandable because $S(\mu)$ for $\mu>0$ is dominated by those high-energy parts of the dipole spectrum which arise from tight inner structures. A fine point to note in this context is a strong curvature of $\log_{10}S(\mu)$ for $\mu>0$, which testifies that the oscillator-strength distribution has a considerable spread at high energies. If the distribution were sharply peaked, we should observe a nearly linear increase of $\log_{10}S(\mu)$. Furthermore, every curve in Fig. 11 should show a logarithmic divergence at $\mu=2.5$, because of the well-known asymptotic behavior $df/dE\sim E^{-3.5}$ so long as an atom has an s electron.

To indicate the reliability of the curves based on our model calculations, we have included in Fig. 11 empirical or otherwise accurate data (shown by circles connected by broken curves) for rare gases. Our HS data agree with accurate data reasonably well for He, and excellently for Ne. The agreement is modest for Ar, but looks close enough (partly because of the logarithmic scale) to make us convinced of the reality of the gross systematics we have discussed. Indeed, our data for Ar depart from accurate data more seriously than those for any other atom for which confident assessment is possible. (We have omitted from Fig. 11 accurate data for loose and intermediate atoms because we presented a thorough comparison in Sec. III.) This departure for Ar arises from the inability of the HS model to produce accurately the dipole oscillator-strength distribution for the $3p\rightarrow d$ channel. This case represents a class of transitions for which this model fails owing primarily to the approximate treatment of exchange,[11,81] and secondarily to the neglect of correlation effects in the initial and final states.[82,83] In Ar, the effect of these approximations is most severe near the first ionization potential so that the errors in the moment $S(\mu)$ are most apparent for $\mu<-1$ as seen in Fig. 11.

Finally, we plan to extend the present work to atoms beyond Ar in order to establish the pattern of behavior of $S(\mu)$ and $L(\mu)$ caused by the filling of the d orbitals.

Note added in proof. W. C. Stwalley [J. Chem. Phys. 54, 4517 (1971)] reexamines the analysis of Ref. 30 in regard to the polarizability of Mg, and obtains $S(-2)=18.75$.

ACKNOWLEDGMENTS

We thank F. E. Cummings, Y.-K. Kim, J. Berkowitz, and H. Bichsel for providing unpublished results. We are also grateful to U. Fano and Y.-K. Kim for their critical reading of an earlier manuscript.

*Work performed under the auspices of the U.S. Energy Research and Development Administration.

†Present address: Stanford Research Institute, Menlo Park, Calif. 94025.

[1]H. A. Bethe and E. E. Salpeter, *Quantum Mechanics of One- and Two-Electron Atoms* (Springer-Verlag, Berlin, 1957).

[2]U. Fano and J. W. Cooper, Rev. Mod. Phys. 40, 441 (1968); 41, 724 (1969).

[3]F. Herman and S. Skillman, *Atomic Structure Calculations* (Prentice-Hall, Englewood Cliffs, N.J., 1963).

[4]J. W. Cooper, Phys. Rev. 128, 681 (1962).

[5]S. T. Manson and J. W. Cooper, Phys. Rev. 165, 126 (1968).

[6]E. J. McGuire, Phys. Rev. 175, 20 (1968).

[7]F. Combet-Farnoux, J. Phys. (Paris) 30, 521 (1969).

[8]E. M. Henry, C. L. Bates, and W. J. Veigele, Phys. Rev. A 6, 2131 (1972).

[9]W. D. Barfield, G. D. Koontz, and W. F. Huebner, J. Quant. Spectrosc. Radiat. Transfer 12, 1409 (1972).

[10]J. H. Scofield, Livermore Laboratory Report UCRL-51326, 1973 (unpublished).

[11]D. J. Kennedy and S. T. Manson, Phys. Rev. A 5, 227 (1972).

[12]S. T. Manson, J. Electron Spectrosc. 1, 413 (1972).

[13]J. A. Ball, J. A. Wheeler, and E. L. Fireman, Rev. Mod. Phys. 45, 333 (1973).

[14]McGuire (Ref. 6) approximates $rV(r)$ by a small set of

straight lines, where $V(r)$ is the Herman-Skillman potential. As a consequence the oscillator strengths of Ref. 6 deviate significantly from those obtained by means of the straightforward numerical solution of the same model potentials. We have made a detailed comparison of our results for Ar with those in Ref. 6 to find the average agreement poor (10–30%). Therefore, we repeated the calculations rather than use those from Ref. 6 in order to avoid artifacts due to the numerical treatment alone.

[15]J. L. Dehmer and R. P. Saxon, Argonne National Laboratory Radiological and Environmental Research Division Annual Report, ANL-8060, Pt. I, p. 102, 1973 (unpublished).

[16]R. J. Bell and A. E. Kingston, Proc. Phys. Soc. Lond. 88, 901 (1966).

[17]F. E. Cummings (unpublished).

[18]W. D. Robb, J. Phys. B 6, 945 (1973).

[19]R. R. Teachout and R. T. Pack, At. Data 3, 195 (1971).

[20]W. J. Stevens and F. P. Billingsley, II, Phys. Rev. A 8, 2236 (1973).

[21]J. Thorhallsson, C. Fisk, and S. Fraga, Theor. Chim. Acta 10, 388 (1968).

[22]J. Lahiri and A. Mukherji, J. Phys. Soc. Japan 21, 1178 (1966); also, see Ref. 19.

[23]A. D. Buckingham and P. G. Hibbard, Symp. Faraday Soc. 2, 41 (1968); also, see Ref. 19.

[24]D. R. Johnston, G. J. Oudemans, and R. H. Cole, J. Chem. Phys. 33, 1310 (1960); also, see Ref. 19.

[25]G. E. Chamberlain and J. C. Zorn, Phys. Rev. 129, 677 (1963); also, see Ref. 19.

[26]M. Cohen, Can. J. Phys. 45, 3387 (1967).

[27]R. A. Alpher and D. R. White, Phys. Fluids 2, 153 (1959).

[28]S. Kaneko and S. Arai, J. Phys. Soc. Japan 26, 170 (1969); also, see Ref. 19.

[29]A. Dalgarno and A. E. Kingston, Proc. R. Soc. A 259, 424 (1960); also, see Ref. 19.

[30]P. L. Altick, J. Chem. Phys. 40, 238 (1964).

[31]S. Hameed, Phys. Rev. A 4, 543 (1971).

[32]M. Inokuti, R. L. Platzman, and Y.-K. Kim, Phys. Rev. 164, 55 (1967).

[33]M. Inokuti, R. P. Saxon, and J. L. Dehmer, Int. J. Radiat. Phys. Chem. 7, 109 (1975).

[34]L. B. Mendelsohn, F. Biggs, and J. B. Mann, Phys. Rev. A 2, 1130 (1970).

[35]C. Froese-Fischer, At. Data 4, 301 (1972).

[36]J.-P. Desclaux, At. Data Nucl. Data Tables 12, 311 (1973).

[37]E. Eggarter, J. Chem. Phys. 62, 833 (1975).

[38]J. Berkowitz (personal communication).

[39]P. Gombás, *Die statistische Theorie des Atoms und ihre Anwendungen* (Springer, Vienna, 1949).

[40]R. J. Bell and A. Dalgarno, Proc. Phys. Soc. Lond. 86, 375 (1965).

[41]R. J. Bell and A. Dalgarno, Proc. Phys. Soc. Lond. 89, 55 (1966). [Note that the $S(-1)$ value given for Rn is erroneous by a factor of 4.]

[42]C. L. Pekeris, Phys. Rev. 115, 1216 (1959).

[43]A. C. Yates and P. W. Langhoff, Phys. Rev. Lett. 25, 1317 (1970).

[44]P. W. Langhoff and A. C. Yates, J. Phys. B 5, 1071 (1972).

[45]L. M. Biberman and G. É. Norman, Ups. Fiz. Nauk 91, 193 (1967) [Sov. Phys.—Usp. 10, 52 (1967)].

[46]G. M. Stacey and A. Dalgarno, J. Chem. Phys. 48, 2512 (1968).

[47]M. Naon, M. Cornille, and Y. -K. Kim, J. Phys. B 8, 864 (1975). See also Y.-K. Kim, M. Naon, and M. Cornille, Argonne National Laboratory Radiological and Environmental Research Division Annual Report, ANL-8060, Pt. I, p. 14, 1973 (unpublished).

[48]R. P. Saxon, Phys. Rev. A 8, 839 (1973).

[49]J. A. Barker and P. J. Leonard, Phys. Lett. 13, 127 (1964).

[50]K. R. Piech and J. S. Levinger, Phys. Rev. 135, A332 (1964).

[51]K. G. Sewell, Phys. Rev. 138, A418 (1965).

[52]I. Shimamura, T. Watanabe, M. Natori, and M. Matsuzawa, in Progress Report VI, Research Group on Atoms and Molecules, Japan, p. 7, 1973 (unpublished).

[53]S. Arai and S. Kaneko, J. Phys. Soc. Jpn. 26, 1562 (1969).

[54]H. Bethe, Ann. Phys. (Leip.) 5, 325 (1930).

[55]U. Fano, Ann. Rev. Nucl. Sci, 13, 1 (1963).

[56]F. Bloch, Z. Phys. 81, 363 (1933).

[57]W. F. Miller, Ph.D. thesis (Purdue University, 1956) (unpublished).

[58]K. L. Bell and A. E. Kingston, Proc. Phys. Soc. Lond. 90, 901 (1964).

[59]Y. M. Chan and A. Dalgarno, Proc. R. Soc. A 285, 457 (1965).

[60]Y. M. Chan and A. Dalgarno, Proc. Phys. Soc. Lond. 86, 777 (1965).

[61]A. Dalgarno, Proc. Phys. Soc. Lond. 76, 422 (1960).

[62]J. D. Garcia, Phys. Rev. 147, 66 (1966).

[63]E. J. McGuire, Phys. Rev. A 3, 267 (1971).

[64]J. E. Turner, P. D. Roecklein, and R. B. Vora, Health Phys. 18, 159 (1970).

[65]C. C. Hanke and H. Bichsel (unpublished).

[66]A. Dalgarno, T. Degges, and D. A. Williams, Proc. Phys. Soc. Lond. 92, 291 (1967).

[67]C. Tschalär and H. Bichsel, Phys. Rev. 175, 476 (1968).

[68]C. C. Hanke and H. Bichsel, K. Dan. Vidensk. Selsk. Mat. -Fys. Medd. 38, No. 3 (1970).

[69]P. L. Altick, Phys. Rev. 169, 21 (1968).

[70]W. K. Chu and D. Powers, Phys. Lett. 40A, 23 (1972). H. Bichsel, and N. S. Laulainen, Bull. Am. Phys. Soc. 16, 842 (1971), report a similar calculation. Because these authors use $\gamma=1$, their results are even closer to our HS values of I_0/Z.

[71]J. Lindhard and M. Scharff, K. Dan. Vidensk. Selsk. Mat. -Fys. Medd. 27, No. 15 (1953).

[72]J. E. Turner, in *Studies in Penetration of Charged Particles in Matter*. National Academy of Sciences Pub. 1133, Nuclear Science Series, Report No. 39 (National Academy of Sciences–National Research Council, Washington, D.C., 1964), pp. 39 and 99.

[73]H. Bichsel, in *American Institute of Physics Handbook*, 3rd ed., edited by D. E. Gray (McGraw-Hill, New York, 1972), Chap. 8d.

[74]P. Dalton and J. E. Turner, Health Phys. 15, 257 (1968).

[75]R. L. Platzman, in *Symposium on Radiobiology. The Basic Aspects of Radiation Effects on Livitg Systems*, edited by J. J. Nickson (Wiley, New York, 1952), p. 139.

[76]M. Inokuti (unpublished). A forthcoming paper will discuss general properties of $\sum_j \sum_{k\neq j} \langle \vec{p}_j \cdot \vec{p}_k \rangle$ and

$\sum_j \sum_{k\neq j} \langle \vec{r}_j \cdot \vec{r}_k \rangle$.
[77]C. J. Kleinman, Y. Hahn, and L. Spruch, Phys. Rev. 165, 53 (1968).
[78]A. Dalgarno, G. W. F. Drake, and G. A. Victor, Phys. Rev. 176, 194 (1968).
[79]P. W. Langhoff and M. Karplus, J. Opt. Soc. Am. 59, 863 (1969).
[80]J. Starkschall and R. G. Gordon, J. Chem. Phys. 54, 663 (1971).
[81]A. F. Starace, Phys. Rev. A 2, 118 (1970).
[82]M. Ya. Amus'ya, N. A. Cherepkov, and L. V. Chernysheva, Zh. Eksp. Teor. Fiz. 60, 160 (1971) [Sov. Phys.—JETP 33, 90 (1971)].
[83]H. P. Kelly and R. L. Simons, Phys. Rev. Lett. 30, 529 (1973).